BAFF-driven B cell hyperplasia underlies lung disease in common variable immunodeficiency

Paul J. Maglione,[1] Gavin Gyimesi,[1] Montserrat Cols,[1] Lin Radigan,[1] Huaibin M. Ko,[2] Tamar Weinberger,[1] Brian H. Lee,[3] Emilie K. Grasset,[1,4] Adeeb H. Rahman,[3] Andrea Cerutti,[1,5,6] and Charlotte Cunningham-Rundles[1]

[1]Division of Clinical Immunology, Department of Medicine, [2]Department of Pathology, [3]Human Immune Monitoring Center, Icahn School of Medicine at Mount Sinai, New York, New York, USA. [4]Experimental Cardiovascular Medicine, Center for Molecular Medicine, Department of Medicine, Karolinska Institutet, Karolinska University Hospital, Stockholm, Sweden. [5]Program for Inflammatory and Cardiovascular Disorders, Institut Hospital del Mar d'Investigacions Mèdiques (IMIM), Barcelona, Spain. [6]Catalan Institute for Research and Advanced Studies (ICREA), Barcelona, Spain.

BACKGROUND. Common variable immunodeficiency (CVID) is the most common symptomatic primary immunodeficiency and is frequently complicated by interstitial lung disease (ILD) for which etiology is unknown and therapy inadequate.

METHODS. Medical record review implicated B cell dysregulation in CVID ILD progression. This was further studied in blood and lung samples using culture, cytometry, ELISA, and histology. Eleven CVID ILD patients were treated with rituximab and followed for 18 months.

RESULTS. Serum IgM increased in conjunction with ILD progression, a finding that reflected the extent of IgM production within B cell follicles in lung parenchyma. Targeting these pulmonary B cell follicles with rituximab ameliorated CVID ILD, but disease recurred in association with IgM elevation. Searching for a stimulus of this pulmonary B cell hyperplasia, we found B cell–activating factor (BAFF) increased in blood and lungs of progressive and post-rituximab CVID ILD patients and detected elevation of BAFF-producing monocytes in progressive ILD. This elevated BAFF interacts with naive B cells, as they are the predominant subset in progressive CVID ILD, expressing BAFF receptor (BAFF-R) within pulmonary B cell follicles and blood to promote Bcl-2 expression. Antiapoptotic Bcl-2 was linked with exclusion of apoptosis from B cell follicles in CVID ILD and increased survival of naive CVID B cells cultured with BAFF.

CONCLUSION. CVID ILD is driven by pulmonary B cell hyperplasia that is reflected by serum IgM elevation, ameliorated by rituximab, and bolstered by elevated BAFF-mediated apoptosis resistance via BAFF-R.

FUNDING. NIH, Primary Immune Deficiency Treatment Consortium, and Rare Disease Foundation.

Conflict of interest: The authors have declared that no conflict of interest exists.

Submitted: June 6, 2018
Accepted: January 25, 2019
Published: March 7, 2019

Reference information:
JCI Insight. 2019;4(5):e122728.
https://doi.org/10.1172/jci.insight.122728.

Introduction

Common variable immunodeficiency (CVID) is the most common symptomatic primary immunodeficiency, affecting about 1 in 25,000 individuals and predisposing to infections that most typically affect the respiratory tract (1). This primary immunodeficiency is defined by marked reduction of serum immunoglobulin G (IgG), IgA, and/or IgM and impaired antibody responses along with arrested memory B cell and plasma cell development (2, 3). CVID is an immune deficiency syndrome resulting from heterogeneous genetic etiologies of which a small fraction are known (4). About half of those with CVID develop chronic inflammatory and/or lymphoproliferative complications for reasons not understood (5). CVID patients with these complications have significantly reduced survival along with markedly worsened morbidity and quality of life (6–8).

Interstitial lung disease (ILD) occurs in 1 out of 3 or more of CVID patients and manifests within the spectrum of benign lymphoproliferative lung pathology, beginning with follicular bronchiolitis, when lymphoproliferation is limited to the peribronchial areas, and expanding to lymphocytic interstitial

pneumonia and nodular lymphoid hyperplasia, when lymphocytic inflammation is more diffuse (9–11). Granulomatous inflammation is often a feature of this form of ILD (11–13). Recurrent or severe lung infections do not explain the development of ILD in CVID, as there is no correlation of ILD with bronchiectasis or pneumonia and IgG replacement therapy does not prevent or treat ILD in most cases (11, 14, 15). Evidence from primary immunodeficiency patients with defined genetic lesions, such as deficiencies of cytotoxic T lymphocyte–associated protein 4 (CTLA-4) or gain-of-function of signal transducer and activator of transcription 3 (STAT3), illustrate that inborn immune dysregulation can underlie the same type of ILD seen in CVID (16–18). ILD is highly associated with autoimmune cytopenias and splenomegaly in CVID, further emphasizing systemic immune dysregulation as a common denominator (19). However, the mechanisms underlying ILD in CVID remain to be defined.

B cells may be a key pathogenic factor in CVID ILD. Pulmonary B cell hyperplasia with formation of tertiary lymphoid structures containing markers of germinal centers is a major pathological characteristic of CVID ILD (20). Further supporting a pathogenic role of B cells in CVID ILD, X-linked agammaglobulinemia patients have profound antibody deficiency like CVID, but do not have B cells and do not develop ILD nearly as frequently (21). B cell–activating factor (BAFF) promotes activation and survival of B cells and has been linked to pathogenic B cell responses that underlie autoimmunity and lymphoid hyperplasia in humans and mice (22). CVID patients have elevated levels of BAFF, but it is not known whether BAFF has a role in driving autoimmune and lymphoproliferative complications in these individuals (23, 24). BAFF can promote the formation of tertiary lymphoid structures in the lungs of patients with chronic pulmonary disease, but whether it has a role in perpetuating these structures that are also present in CVID ILD is not known (25, 26).

With the goal to improve understanding of the pathogenesis of CVID ILD, we interrogated the clinical and laboratory parameters of our patient cohort aiming to identify a biomarker that distinguishes those with ILD progression. We found elevation of serum IgM to be associated with progressive ILD in CVID, a biomarker that reflected the extent of pulmonary B cell follicle formation. This B cell hyperplasia can be targeted by rituximab leading to amelioration of CVID ILD. However, progressive CVID ILD was prone to recurrence and associated with elevated levels of BAFF in the lungs and serum. We found this disease process to be supported by BAFF-driven apoptosis inhibition primarily mediated through BAFF receptor (BAFF-R) and its induction of Bcl-2. This identification of a serum biomarker and what we believe is a novel pathway of disease pathogenesis in CVID ILD provides an opportunity to optimize patient selection and timing of B cell–depletive treatment as well as highlights a BAFF-driven pathogenic mechanism that should be further evaluated to improve treatment of these patients and others with pathologically similar ILD.

Results

Increase of serum IgM distinguishes CVID patients with progressive ILD. We previously reported that ILD can be stable or progressive in CVID and used pulmonary function testing (PFT) to define progressive ILD as a decrease in the percentage predicted forced vital capacity (FVC) of 10 or greater or diffusion capacity of the lungs for carbon monoxide (DLCO) of 15 or greater within a 20-month period based on American Thoracic Society criteria (27, 28). We also found higher serum IgM, but not other conventional laboratory parameters, to distinguish those with progressive ILD from other CVID patients (28). We set out to explore the relationship between serum IgM and CVID ILD.

First, we validated the findings of the previous study in a larger 73-CVID-patient cohort followed at the Mount Sinai Clinical Immunology Faculty Practice. This CVID cohort consisted of 44 patients without ILD as well as 14 patients with stable ILD and 15 with progressive ILD (Figure 1A). Within this CVID cohort, there was no significant difference in age or sex predominance and the only clinical characteristic that differed was that immune thrombocytopenic purpura (ITP) occurred more often in those with ILD (Table 1), as previously reported (11). Other than 3 patients in the progressive ILD group who had mutations in *TNFRSF13B*, the gene encoding transmembrane activator and CAML interactor (TACI), no other known pathogenic mutations were found by whole-exome sequencing in our CVID cohort (29).

We found that CVID patients with progressive ILD had significantly greater elevation of serum IgM than other CVID patients (Figure 1B). Changes in other laboratory parameters, including serum IgA as well as leukocyte and lymphocyte subset levels were not significantly different (Supplemental Figure 1; supplemental material available online with this article; https://doi.org/10.1172/jci.insight.122728DS1).

Table 1. Characteristics of the study population (*n* = 73)

	No ILD	Stable ILD	Progressive ILD	*P* value[A]
Number of Subjects	44	14	15	
Female (%)	24 (55)	8 (57)	10 (67)	0.714
Median Age (95% CI)	52 (50–60)	49 (44–59)	48 (40–52)	0.189
Subjects (%) with history of:				
Pneumonia	27 (61)	10 (71)	8 (53)	0.605
Bronchiectasis	8 (18)	7 (50)	4 (29)	0.061
ITP	2 (4.5)	10 (71)	14 (93)	**<0.0001**
Other autoimmunity	2 (4.5)	2 (14)	3 (20)	0.172
Median Lab Value (95% CI)				
Diagnostic IgG (mg/dl)	210 (174–249)	100 (69–240)	157 (102–288)	0.226
Diagnostic IgA (mg/dl)	7 (7–17)	2 (0–15)	5 (2–7)	0.295
Diagnostic IgM (mg/dl)	11 (12–22)	20 (10–39)	15 (10–46)	0.613
WBC (10^3/μl)	5.5 (5.4–6.4)	5.6 (4.8–8.0)	5.7 (4.3–7.9)	0.835
Neutrophils (10^3/μl)	3.5 (3.3–4.2)	3.8 (3.2–4.8)	4.4 (2.7–5.1)	0.646
Monocytes (10^3/μl)	0.5 (0.3–1.1)	0.4 (0.3–0.6)	0.4 (0.3–0.8)	0.095
$CD4^+$ T cells (/μl)	602 (511–839)	552 (344–956)	610 (431–816)	0.951
$CD8^+$ T cells (/μl)	339 (363–622)	273 (161–713)	252 (170–438)	0.145
$CD19^+$ B cells (/μl)	173 (143–262)	69 (13–379)	79 (41–157)	0.090

[A]Categorical values were compared using the χ^2 test. Continuous values were compared using the Kruskal-Wallis test. ILD, interstitial lung disease; ITP, immune thrombocytopenic purpura; WBC, white blood cell.

We chose to focus on change in serum IgM, rather than absolute IgM level, because focusing on the increase in IgM overcomes heterogeneity of absolute IgM levels in CVID (Table 1). All patients were on IgG replacement therapy and thus changes in IgG levels were not examined. Patients with serum IgM increase of 10 mg/dl or greater, a value determined to be outside of normal variation for CVID, had significantly greater decreases in FVC (Figure 1C) and DLCO (Figure 1D) after 12 and 24 months. Together, these data identified serum IgM increase as a biomarker of ILD progression in CVID.

We sought to validate our association of serum IgM elevation with ILD progression in another patient cohort. The United States Immunodeficiency Network (USIDNET) maintains a registry of clinical and laboratory data on primary immunodeficiency patients from more than 45 geographically diverse institutions in the United States and Canada. While the USIDNET registry does not contain PFT data and we could not stratify CVID ILD as stable or progressive, there were 200 non–Mount Sinai CVID patients for which 2 or more values for serum IgM at least 6 months apart were available. A serum IgM increase of 10 mg/dl or more was found in 50% of the 28 non–Mount Sinai CVID ILD patients in the USIDNET registry compared with only 18% of non–Mount Sinai CVID patients in the registry that were not reported to have ILD (Figure 1E). Moreover, the serum IgM increase in CVID ILD patients in the registry was significantly greater than the serum IgM change observed in CVID patients without ILD (Figure 1F). Thus, USIDNET data demonstrate that serum IgM increase occurs in a greater proportion and to a greater extent in CVID patients with ILD compared to those without ILD, supporting serum IgM increase as a biomarker of CVID ILD progression.

Serum IgM increase reflects B cell hyperplasia and local IgM production in CVID ILD. As ectopic B cell follicles are a feature of CVID ILD (20), we speculated that the prevalence of these follicles may relate to the serum IgM increase we observed. Ectopic B cell follicles in CVID ILD lung biopsy sections express the B cell marker CD20 along with markers of tertiary lymphoid structures (CD23 for follicular dendritic cells, CD3 for T cells, Bcl6 and Ki67 for germinal centers) (Figure 2A). Ectopic B cell follicles from all CVID ILD biopsies were determined to be polyclonal, utilizing Ig light chain kappa and lambda immunohistochemistry and/or polymerase chain reaction. Ectopic B cell follicles in CVID ILD biopsies were quantified and then correlated with serum IgM levels in a blinded manner. Serum IgM levels were higher in those with more numerous ectopic B cell follicles, indicating that serum IgM reflects the degree of pulmonary B cell hyperplasia (Figure 2B).

Upon noting that IgM levels correlated with ectopic B cell follicles in CVID ILD, we examined whether IgM was being produced by these pulmonary B cells. The ectopic B cell follicles expressed IgM

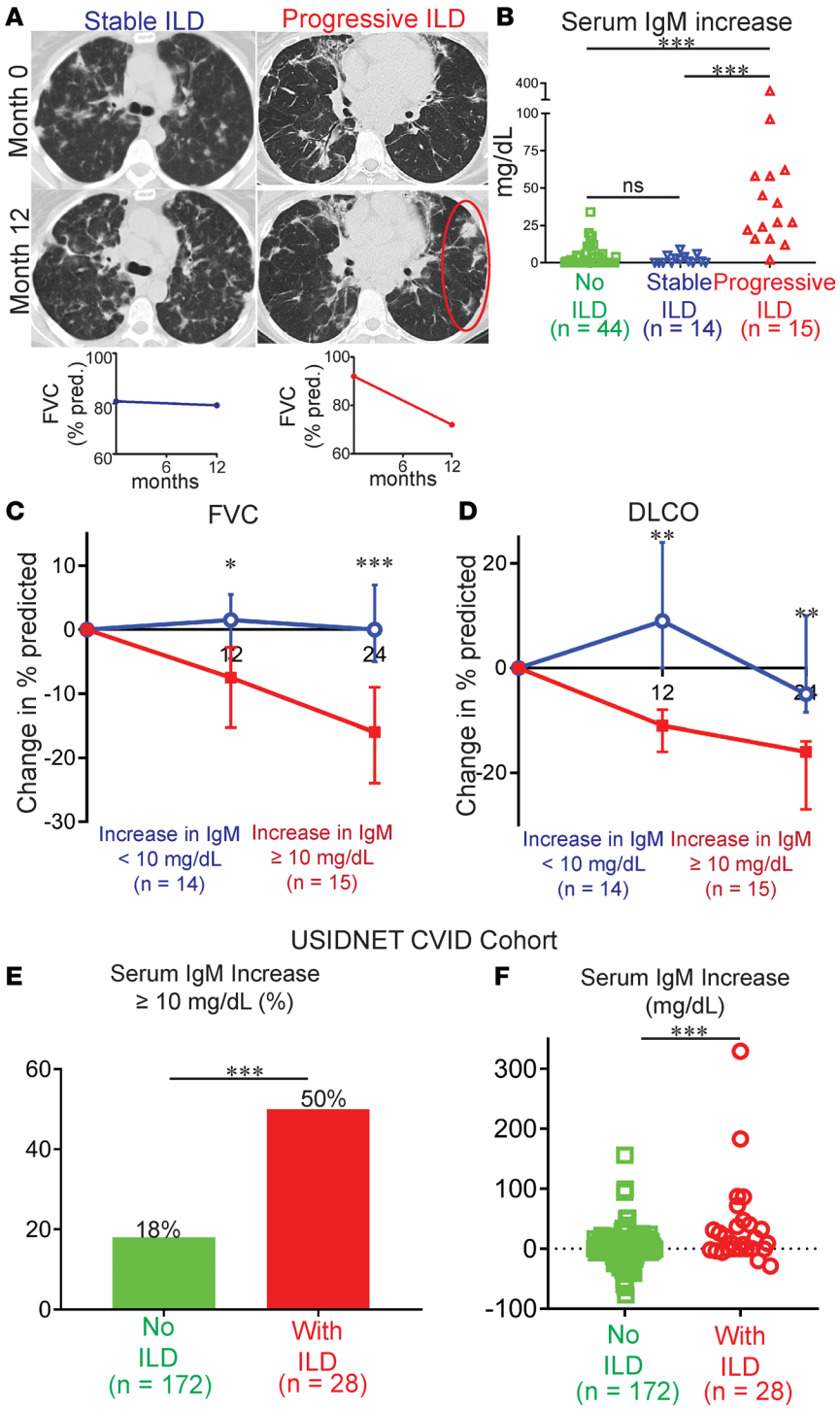

Figure 1. Increase of serum IgM distinguishes CVID patients with progressive ILD. (**A**) CT chest scans from CVID patients with stable or progressive ILD over a 12-month period (area of worsening inflammation is circled) and corresponding FVC measurements. (**B**) Serum IgM increased to a significantly higher level in CVID patients with progressive ILD compared with those with stable or no ILD over 24 months of followup. (**C**) FVC and (**D**) DLCO over 24 months measured in CVID ILD patients grouped on the basis of serum IgM increase ≥ or < 10 mg/dl. (**E**) A greater proportion of CVID ILD patients had a serum IgM increase of ≥ 10 mg/dl compared with other CVID patients in the USIDNET registry. (**F**) Serum IgM increased to a significantly higher level in CVID patients with ILD compared with those without in the USIDNET registry. $^{*}P < 0.05$, $^{**}P < 0.01$, $^{***}P < 0.001$ by Kruskal-Wallis test for 3-group comparison and Mann-Whitney test for 2-group comparison. ns, not significant.

and IgD, but not IgG, while extrafollicular B cells brightly expressed IgM, suggesting high cytoplasmic IgM that, together with the CD38 expression we also observed, is characteristic of plasmablasts (Figure 2C). CVID ILD patients with large increases in serum IgM had numerous IgM^+ B cells in and around ectopic pulmonary follicles, while those with stable serum IgM levels did not (Figure 2D). We quantified this observed difference in lung biopsies from 13 CVID ILD patients (2 non-serial sections per patient), finding that CVID ILD patients with a change in serum IgM of 10 mg/dl or greater had significantly more IgM^+ cells in the lungs, even when accounting for an increase in total cells (Figure 2E). These data demonstrate that the serum IgM increase we observed in CVID patients with progressive ILD reflects not only the extent of pulmonary B cell hyperplasia but also the IgM production within and adjacent to these ectopic B cell follicles.

Rituximab improves PFT and suppresses serum IgM in CVID ILD, but disease recurs in association with IgM elevation. As we found progressive ILD to be associated with greater extent and IgM production of pulmonary B cell hyperplasia, we treated 11 subjects with progressive ILD with rituximab. All patients treated with rituximab had an increase in FVC and their ILD progression stabilized or improved over the next 12 months (Figure 3A). The change in FVC in the rituximab-treated patients was significantly greater than that which occurred during the natural course of the 22 patients with ILD that either did not receive rituximab or had PFT values measured for at least 12 months prior to receiving rituximab, including patients that met both progressive and stable ILD criteria. All patients, whether or not they were treated with rituximab, received supportive care that included Ig replacement, inhaled corticosteroids, and antibiotics but no additional immunomodulatory therapy. DLCO was also significantly improved by rituximab compared with CVID ILD patients receiving supportive care (Figure 3B). Serum IgM levels were dramatically reduced by rituximab in association with these PFT improvements (Figure 3C). Thus, rituximab is effective for the treatment of CVID ILD in association with depletion of serum IgM.

The 3 patients with TACI mutations included in this study all had progressive ILD and received rituximab (marked in red in Figure 3, A–C). Two of the patients were heterozygous for the C104R TACI mutation while the other had compound heterozygous damaging mutations (C104R, S194X). The patient with compound heterozygous mutations showed modest improvement with rituximab followed by recurrence characterized by a higher IgM level and more extensive pulmonary inflammation on CT than prior to therapy (Figure 3D). This suggested that biallelic loss of TACI may impart greater resistance and/or more robust recurrence after rituximab as well as indicates a potential role of its ligand BAFF in the progression of CVID ILD.

Four of the 11 rituximab-treated patients (36.4%) developed recurrence of progressive ILD within 18 months, as defined by pulmonary function decline of 10% predicted (Figure 3E). Correspondingly, 3 of the 9 rituximab-treated patients (33.3%) who had DLCO values measured also demonstrated progressive ILD recurrence as evidenced by a decline of greater than 15% predicted in DLCO (Figure 3F). Noted in blue are the 4 patients who received additional therapy with azathioprine initiated 6 months after receiving rituximab at the discretion of the treating physician. Serum IgM increase correlated with FVC decline after rituximab ($r = –0.79$) (Figure 3G). Our results indicate that B cell–depletive therapy ameliorates CVID ILD; however, recurrence occurs in a significant subset of patients in association with serum IgM increase after rituximab.

BAFF is elevated in CVID patients with progressive ILD and correlates with STAT1 expression. As recurrence after rituximab has been linked with elevation of BAFF in systemic lupus erythematosus (SLE) and Sjogren's syndrome (30, 31), we measured levels of BAFF as well as APRIL (a proliferation-inducing ligand), the cytokine that shares 2 receptors with BAFF and also promotes activation of B cells. We found BAFF to be significantly increased in serum of CVID patients with progressive ILD compared with CVID patients with stable ILD, CVID without ILD, and healthy controls (Figure 4A). We also found BAFF significantly elevated in CVID ILD patients that received rituximab or had mutation of TACI, which we analyzed separately because TACI is a receptor for BAFF. We did not find significant differences in serum levels of APRIL. Correspondingly, we detected BAFF in the lung biopsies from CVID patients with progressive ILD more prominently than those with stable ILD (Figure 4B). We found $BAFF^+$ cells, but not total cells ($DAPI^+$), to be increased in progressive ILD patients compared with stable ILD or non–CVID ILD pulmonary lymphoid hyperplasia controls. These results indicate that elevated BAFF in the blood as well as the lungs distinguishes CVID patients with progressive ILD.

One hypothesis for the BAFF elevation we observed is that receptors for BAFF are reduced in CVID due to the B cell maturation defect inherent to these patients. BAFF-R is expressed at all stages of B cell development, while the expression of TACI and B cell maturation antigen (BCMA), the third receptor for BAFF, increases in conjunction with maturation into memory and antibody-producing cells, a maturation that is impaired by CVID (32). In accordance with the expression of these receptors on more mature B cell subsets that are absent in CVID, TACI and BCMA expression was reduced in whole blood from CVID patients relative to healthy controls using publicly available RNA expression data (NCBI GEO accession GSE51405) (Figure 4D) (33). This RNA expression data set is from the Mount Sinai CVID cohort and is linked with information about ILD as well as other noninfectious complications. There was no difference in TACI and BCMA expression between the stable and progressive ILD groups, so this could not explain the differences in BAFF we observed. Elevations of IFN-γ and IFN-γ–producing cells in the blood have been associated with inflammatory complications in CVID (33–35). We found plasma IFN-γ to be higher in CVID patients with progressive ILD compared with CVID patients with stable or no ILD (Supplemental Figure 2).

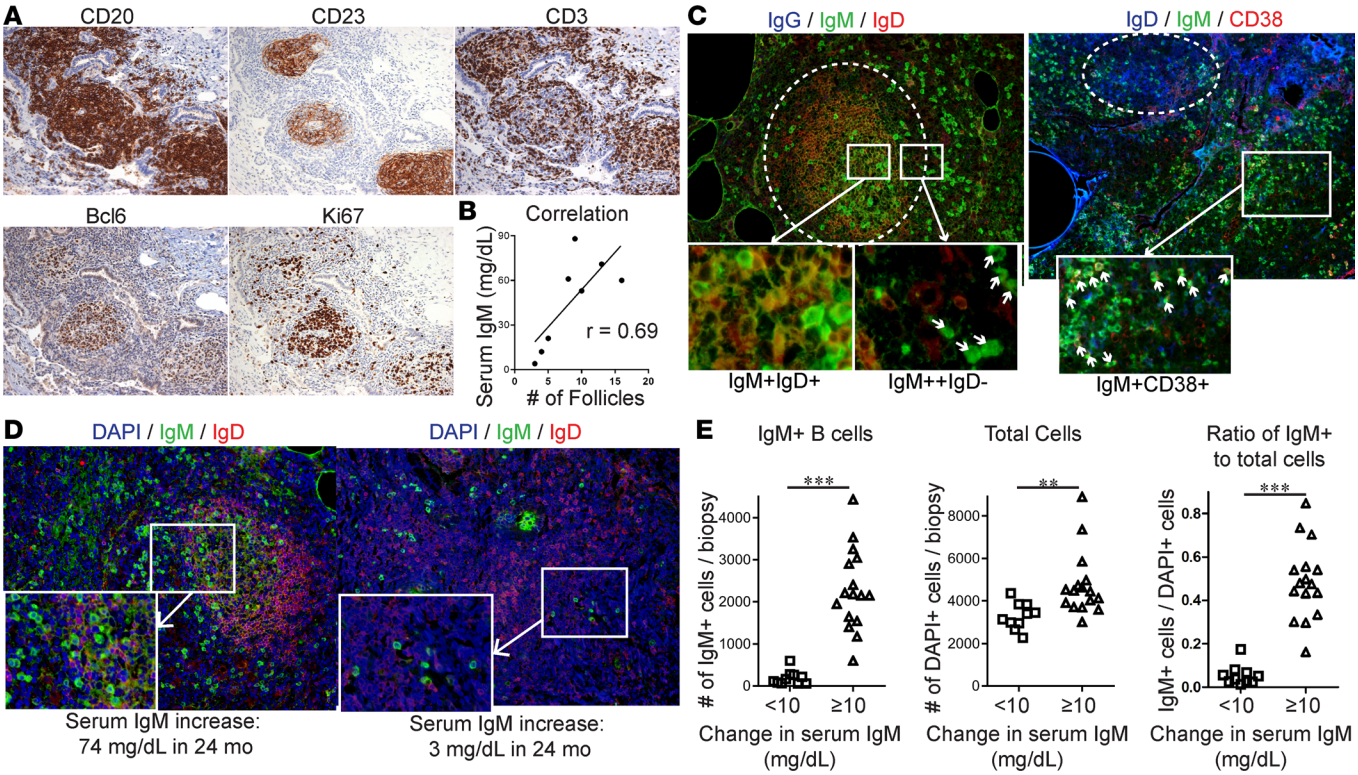

Figure 2. Serum IgM increase reflects B cell hyperplasia and local IgM production in CVID ILD. (**A**) CD20$^+$CD23$^+$CD3$^+$Bcl6$^+$Ki67$^+$ ectopic B cell follicles (serial sections from the same patient, ×200 magnification) in CVID ILD biopsies were quantified and (**B**) correlated with serum IgM (Spearman's $r = 0.69$) in 8 patients. (**C**) These ectopic B cell follicles in CVID patients expressed IgM and IgD, but not IgG, and extrafollicular IgM^{bright}IgD$^-$CD38$^+$ plasmablasts were also identified (marked with white arrows). Larger images of ×200 magnification with ×1,600 and ×400 magnification insets, respectively. Data representative of those from 6 subjects. (**D**) Representative images showing that lung biopsies from CVID patients with greater serum IgM increase over 24 months had more IgM$^+$ cells in the lungs. Original magnification, ×200 and ×400 (insets). (**E**) Quantification of IgM$^+$ cells of lung biopsies from 13 CVID ILD patients (5 stable ILD, 8 progressive ILD) in which lung tissue was available (2 non-serial sections from each patient included) demonstrated significantly greater IgM$^+$ B cells, total cells (DAPI$^+$), and ratio of IgM$^+$ cells to total cells in progressive ILD patients with serum IgM increase ≥ 10 mg/dl compared with those with stable ILD as quantified using CellProfiler software. $^{**}P < 0.01$, $^{***}P < 0.001$ by Mann-Whitney test.

As IFN-γ is known to drive BAFF production (36), we examined RNA expression of STAT1 because the IFN-γ receptor signals via this transcription factor and upregulates its expression (37). We found STAT1 expression to be highest in the peripheral blood of CVID patients with progressive ILD (Figure 4E) and its expression correlated with that of BAFF ($r = 0.70$) (Figure 4F). Thus, elevation of IFN-γ is a likely stimulus for the elevated BAFF in progressive CVID ILD.

CD14$^+$ monocytes are a prominent source of BAFF in CVID ILD. Our data suggested that BAFF production was driven by IFN-γ in a STAT1-dependent manner. We confirmed that IFN-γ stimulation induced BAFF production by PBMCs from CVID patients and found that IFN-γ–stimulated BAFF production was highest in CVID patients with ILD (Supplemental Figure 3). We then used mass cytometry to identify all major leukocyte subsets in peripheral blood and to find those most responsive to IFN-γ stimulation on the basis of phosphorylated STAT1 (p-STAT1) expression (see Supplemental Figure 4 for markers used to define each leukocyte subset by mass cytometry). We found p-STAT1 expression to be highest in monocyte subsets (CD14$^+$CD16$^-$, CD14$^+$CD16$^+$, and CD16^{hi}) and dendritic cells, with levels that were higher in CVID patients with progressive ILD than in CVID patients with stable or no ILD as well as healthy controls (Figure 5A). We then determined via mass cytometry that the leukocyte subsets expressing the highest p-STAT1, dendritic cell and monocyte subsets, also had the highest levels of intracellular BAFF (Figure 5B). CD14$^+$CD16$^-$ monocytes were by far the most abundant p-STAT1$^+$BAFF$^+$ leukocyte and their frequency in the blood was significantly elevated in CVID patients with progressive ILD compared with other CVID patients and healthy controls (Figure 5C). Moreover, the proportion of CD14$^+$ monocytes producing BAFF was increased in CVID with progressive ILD compared with those with stable or no ILD and healthy controls, as quantified by mass cytometry and confirmed by flow cytometry (Figure 5D).

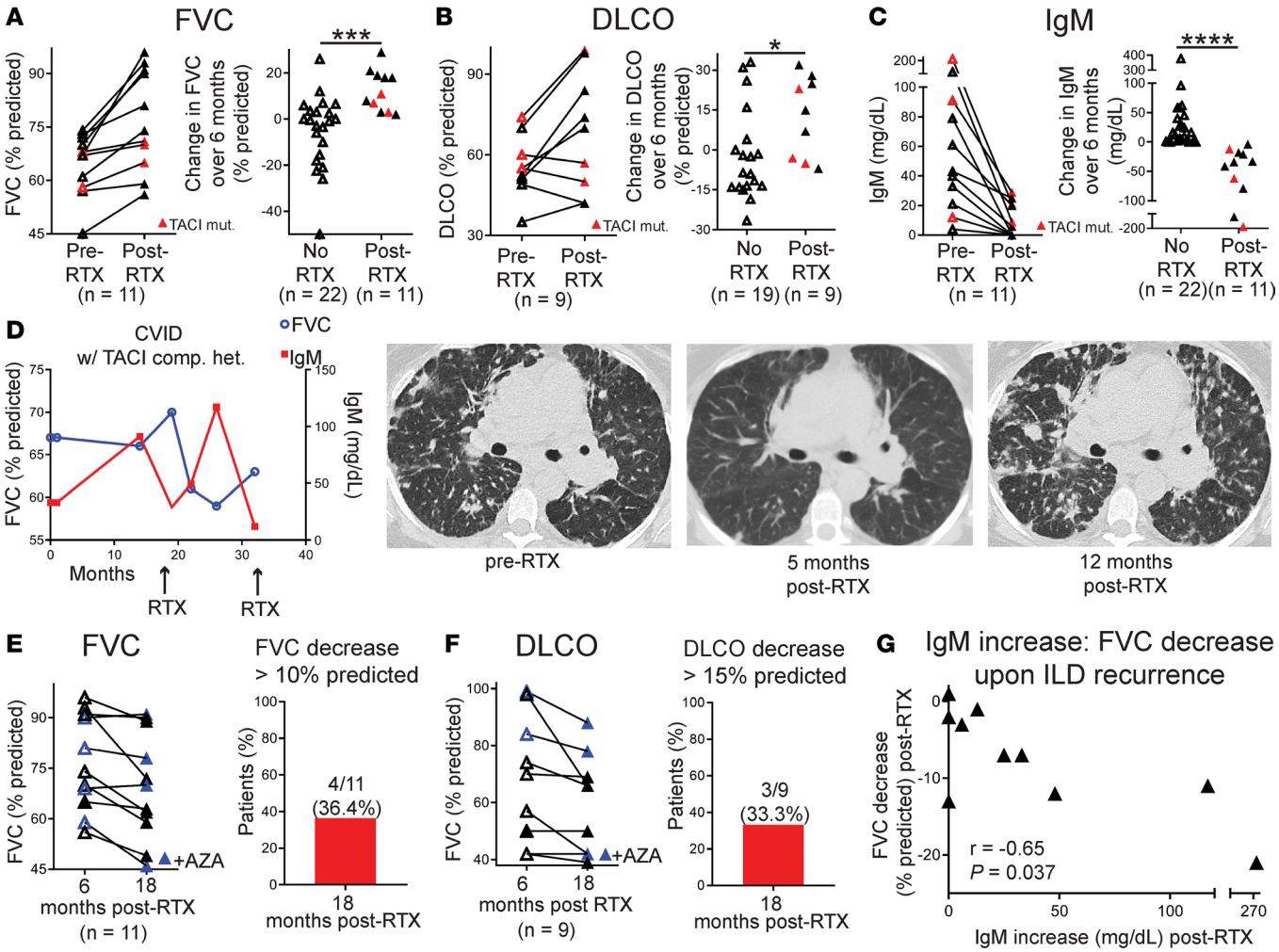

Figure 3. Rituximab improves PFT and suppresses serum IgM in CVID ILD, but disease recurs in association with IgM elevation. (**A**) FVC and (**B**) DLCO were significantly improved in the 11 patients who received rituximab (RTX) compared with the 22 CVID ILD patients followed for 12 months on supportive care. Patients with TACI mutations (TACI mut.) denoted in red. (**C**) Serum IgM levels were dramatically reduced after rituximab compared with CVID ILD patients receiving supportive care. (**D**) FVC and serum IgM levels plotted simultaneously over time in a CVID ILD patient with compound heterozygous TACI mutations. RTX indicates time points when therapy was initiated. (**E**) Progressive CVID ILD recurred within 18 months of RTX in 36.4% of patients by FVC criteria and (**F**) 33.3% of the 9 patients for which DLCO criteria could be assessed. Patients who received azathioprine (AZA) denoted in blue. (**G**) Larger IgM increase correlated with larger FVC decrease after RTX (Spearman's $r = -0.65$, $P = 0.037$). $^*P < 0.05$, $^{***}P < 0.001$, $^{****}P < 0.0001$. Two-group comparison by Mann-Whitney test.

We then confirmed the presence of CD14$^+$ monocytes producing BAFF in CVID ILD biopsies using immunofluorescence (Figure 5E). While we found CD11c$^+$ dendritic cells to be a source of BAFF by mass cytometry, there was no difference in the frequency of these cells in the blood (Figure 5C) and the proportion of BAFF-producing dendritic cells was not different between groups (Figure 5F). Together, these results implicate IFN-γ–responsive CD14$^+$ monocytes as a primary source of BAFF in CVID ILD.

BAFF-R$^+$IgD$^+$ naive B cells predominate in pulmonary follicles and blood in CVID ILD. We next focused on whether BAFF-R and/or TACI (as BCMA expression was absent in CVID ILD, Figure 4C) mediated BAFF effects in CVID ILD. We found BAFF-R to be prominently expressed by the ectopic B cell follicles in CVID ILD, while TACI expression was detectable in extrafollicular areas (Figure 6A). Ectopic B cell follicles were made up of IgM$^+$IgD$^+$CD27$^-$ naive B cells, whereas extrafollicular areas contained IgM^{bright}IgD$^-$ cells expressing the plasmablast markers CD38 and CD27 (Figure 6, B and C). These extrafollicular areas also expressed Ki67 and CD20, further suggesting the IgM-producing cells are plasmablasts rather than plasma cells that do not express these markers (Supplemental Figure 5). IgM$^+$CD38$^+$CD27$^-$ cells were observed within the ectopic B cell follicles, indicative of transitional B cells (Figure 6C). These results identified BAFF-R as the major receptor for BAFF in CVID ILD ectopic B cell follicles that consist predominantly of naive and transitional B cells, while TACI is more highly expressed in extrafollicular areas that likely harbor IgM-producing plasmablasts.

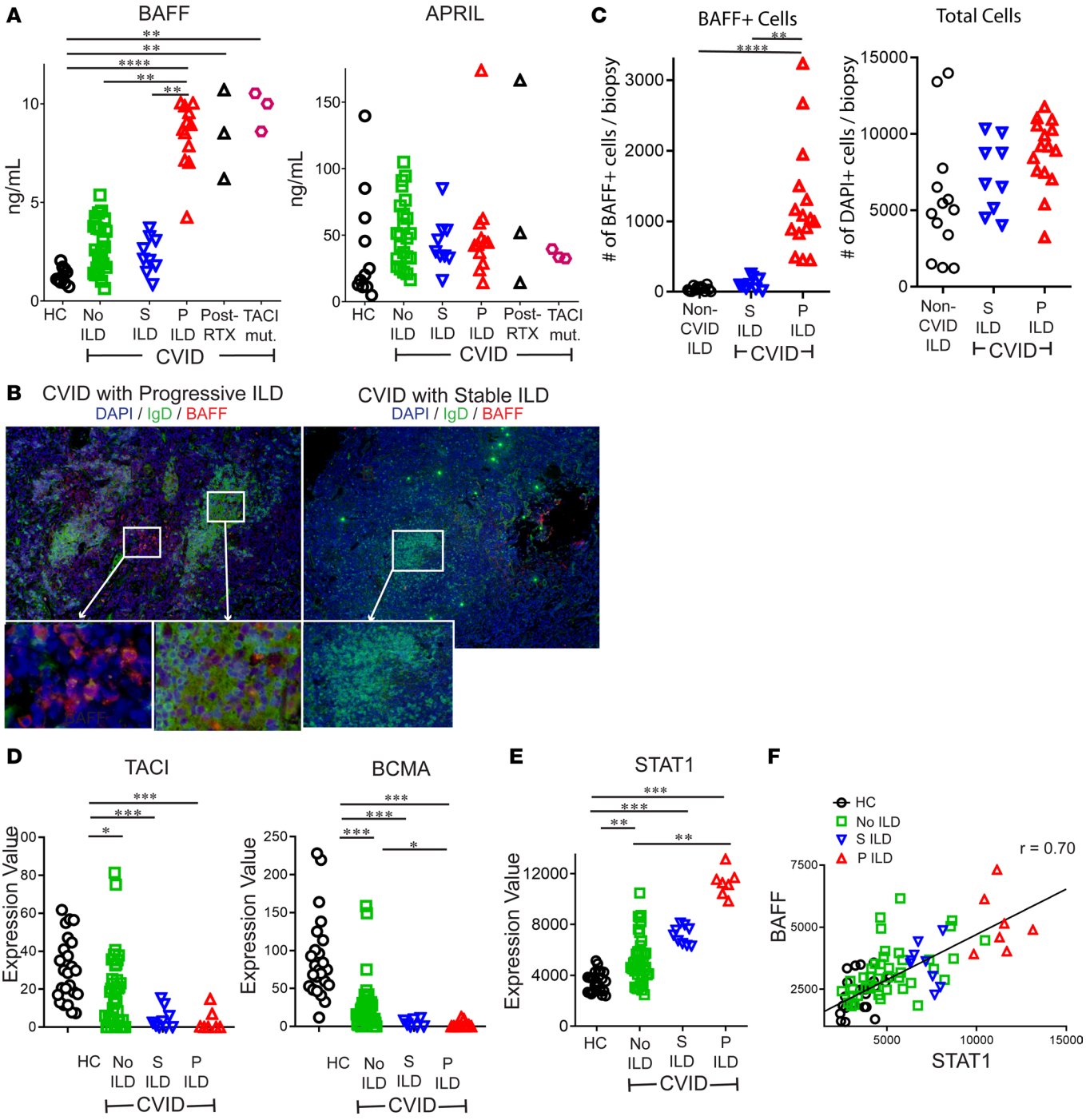

Figure 4. BAFF is elevated in CVID patients with progressive ILD and correlates with *STAT1* expression. (**A**) Serum BAFF, but not APRIL, was significantly increased in CVID patients with progressive (P) ILD compared with CVID with stable (S) ILD, no ILD, and healthy controls. Serum BAFF was also elevated in those treated with rituximab (RTX) and CVID ILD patients with TACI mutations (TACI mut.). (**B**) Immunofluorescence staining of lungs detected BAFF more prominently in patients with P ILD compared with those with S ILD. Figure representative of results from 2 non-serial sections from 6 patients. Original magnification: P ILD, ×200 and ×400 (insets); S ILD, ×100 and ×200 (insets). (**C**) Lung biopsies from 6 CVID patients with P ILD, 4 with S ILD, and 5 patients non–CVID ILD pulmonary lymphoid hyperplasia (2–3 non-serial sections from each patient) demonstrated significantly greater BAFF$^+$ cells, but not total cells (DAPI$^+$) in CVID P ILD. (**D**) RNA expression of *TNFRSF13B* (TACI) and *TNFRSF17* (BCMA) is reduced in CVID patients compared with controls but does not distinguish those with P or S ILD. (**E**) *STAT1* expression was highest in CVID P ILD patients and (**F**) correlated (Spearman) with expression of *TNFSF13B* (BAFF). *P < 0.05, **P < 0.01, ***P < 0.001 by Kruskal-Wallis test for 3-group comparison and Mann-Whitney test for 2-group comparison.

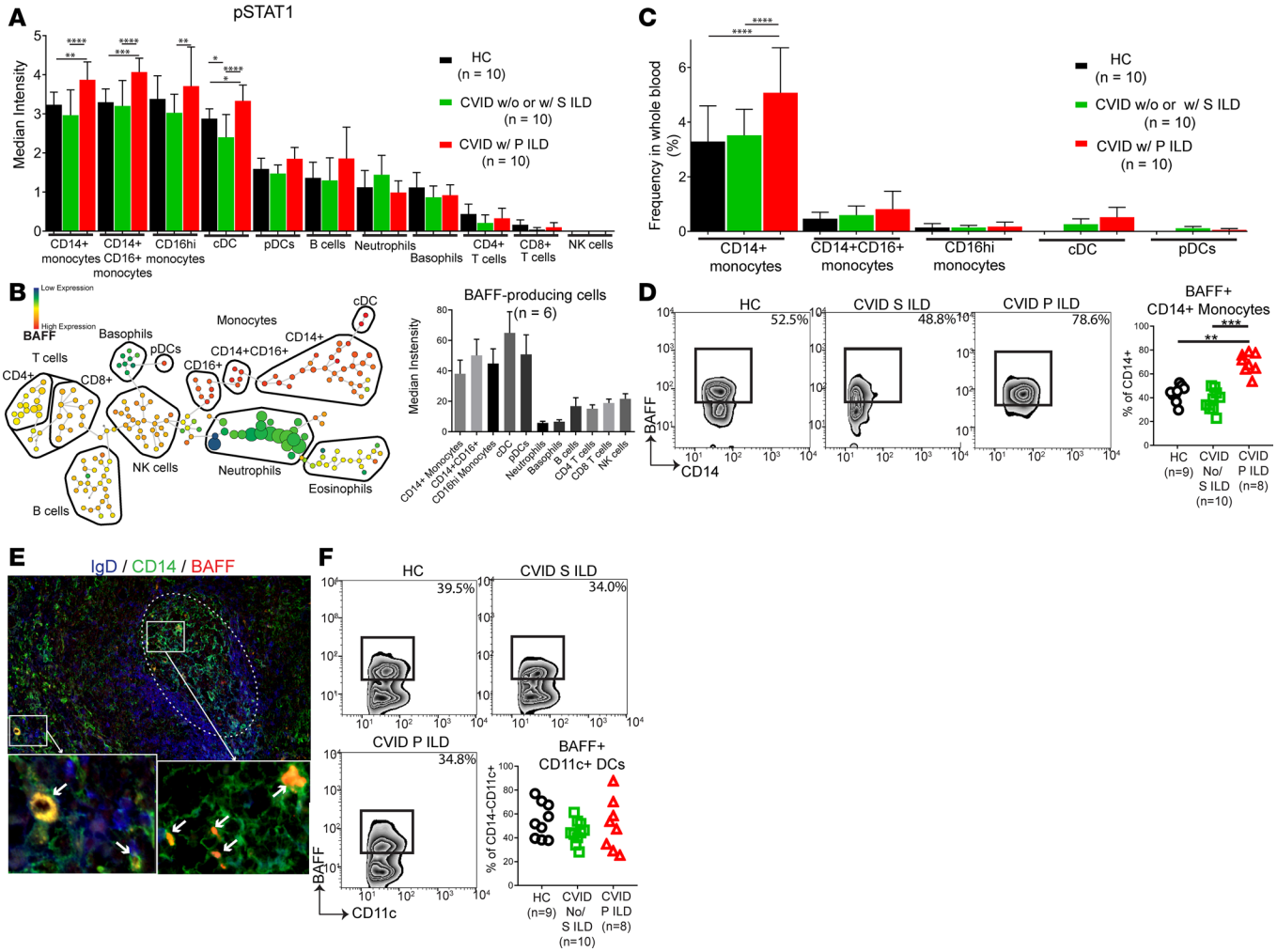

Figure 5. CD14⁺ monocytes are a prominent source of BAFF in CVID ILD. (**A**) Whole blood was analyzed by mass cytometry, showing the highest phosphorylated STAT1 (p-STAT1) in monocytes and dendritic cells of CVID with progressive (P) ILD. CVID patients with no ILD and stable (S) ILD were grouped together because the cost of mass cytometry limited the number of samples that could be done and there was no difference in serum BAFF or STAT1 expression between these groups. (**B**) Monocyte and dendritic cells express the highest levels of intracellular BAFF in CVID ILD as detected by mass cytometry of 6 subjects. Displayed as density-normalized events (left) and plot of median intensity (right). (**C**) $CD14^+CD16^-$ monocytes are elevated in CVID P ILD patients compared with CVID patients with stable (S) or no ILD and healthy controls (HCs), making $CD14^+$ monocytes the most prevalent BAFF-producing subset. (**D**) A greater proportion of $CD14^+$ monocytes produce BAFF in CVID P ILD compared with other CVID patients and controls. (**E**) Immunofluorescence of CVID ILD biopsies identified $CD14^+$ monocytes as sources of BAFF in the lungs (white arrows). IgD^+ B cell follicle highlighted with dotted white circle. Immunofluorescence shown is representative of 3 non-serial sections of lung biopsies from 3 CVID ILD patients. Original magnification, ×200 and ×1,600 (insets). (**F**) There was no difference in the proportion of $lineage^-CD11c^+$ dendritic cells producing BAFF between groups. $^*P < 0.05$, $^{**}P < 0.01$, $^{***}P < 0.001$, $^{****}P < 0.0001$. Error bars represent standard deviation. Multiple group comparison by Kruskal-Wallis test.

We used flow cytometry to measure B cell subsets in the circulation of CVID patients (see Supplemental Figure 6 for gating strategy). In concert with their prominence in the lungs, circulating levels of naive and transitional B cells were highest in the blood of CVID patients with progressive ILD compared with those with stable or no ILD as well as healthy controls (Figure 6D). Levels of circulating $CD27^+CD38^+$ cells, a subset containing the plasmablast population, were similar between all CVID groups and healthy controls (Figure 6E). This was consistent with our observation of $IgM^+CD27^+CD38^+$ cells in CVID ILD lungs and elevation of serum IgM. We confirmed that $CD138^+$ plasma cells were absent from our CVID ILD patients (Supplemental Figure 7), demonstrating that these putative IgM plasmablasts developed in the setting of profound plasma cell deficiency that defines CVID. Isotype-switched memory B cells were significantly reduced in CVID patients with progressive ILD compared with those without ILD and healthy controls (Figure 6F). We found BAFF-R to be reduced on naive and transitional B cells from CVID patients with progressive ILD (Figure 6G), consistent with prior reports of BAFF-R internalization upon BAFF engagement occurring in

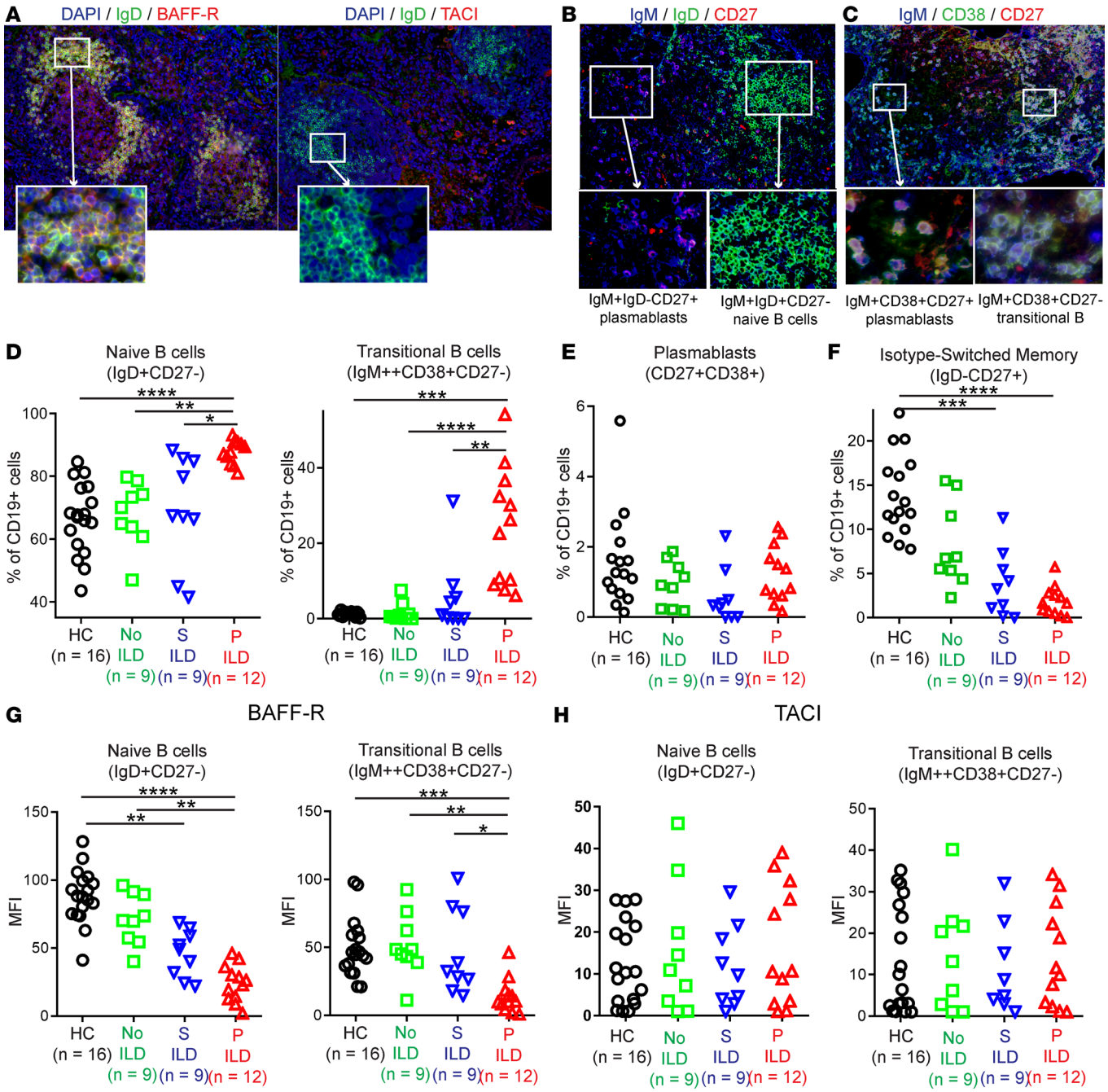

Figure 6. BAFF-R$^+$IgD$^+$ naive B cells predominate in pulmonary follicles and blood in CVID ILD. (**A**) Immunofluorescence of CVID ILD demonstrated prominent BAFF-R expression within IgD$^+$ ectopic B cell follicles, whereas TACI expression was detected in extrafollicular areas. Images shown are representative of data from 6 CVID ILD patients. Original magnification, ×200 and ×400 (insets). (**B** and **C**) The extrafollicular areas were characterized by IgM$^+$IgD$^-$ CD27$^+$CD38$^+$ plasmablasts, while the follicles consisted of mostly IgM$^+$IgD$^+$ naive B cells and IgM$^+$CD38$^+$CD27$^-$ transitional B cells. Original magnification, ×200, ×1,600 (insets in **B**), and ×400 (insets in **C**). (**D**) Progressive (P) ILD patients had significantly elevated circulating naive and transitional B cells compared with CVID patients with stable (S) or no ILD and healthy controls (HCs). (**E**) Levels of circulating CD19$^+$CD27$^+$CD38$^+$ plasmablasts were similar among groups. (**F**) IgD$^-$CD19$^+$CD27$^+$ isotype-switched memory B cells were significantly decreased in CVID patients with S or P ILD compared with HCs and significantly lower in P ILD patients compared with CVID patients without ILD. (**G**) BAFF-R expression by naive and transitional B cells is reduced in CVID patients with P ILD but (**H**) TACI expression is unchanged. *P < 0.05, **P < 0.01, ***P < 0.001, ****P < 0.0001. Multiple group comparison by Kruskal-Wallis test.

high BAFF settings (24). We found no significant differences in TACI expression by naive or transitional B cells among the subject groups (Figure 6H). Together, these data demonstrate that BAFF-R$^+$ naive and transitional B cells predominate in CVID ILD B cell follicles, BAFF engages these B cell subsets via BAFF-R, and TACI expression is limited to extrafollicular areas where the putative IgM$^+$ plasmablasts reside.

Naive B cells express Bcl-2 in response to BAFF-R signaling to resist apoptosis and promote progression of CVID ILD. BAFF-R is distinguished from the other 2 receptors for BAFF, TACI and BCMA, by signaling via the noncanonical NF-κB pathway and inducing expression of Bcl-2 to impair apoptosis (38). Consistent with BAFF-R signaling in CVID ILD, we found BAFF-R and Bcl-2 colocalized within IgD^+ B cell follicles in the lungs (Figure 7A). We also found Bcl-2 expression significantly elevated in freshly isolated circulating naive B cells from CVID progressive ILD patients compared with CVID patients with stable or no ILD and healthy controls (Figure 7B). As further evidence of BAFF-R–mediated noncanonical NF-κB signaling in CVID ILD, we found increased expression of RelB in whole blood of CVID patients with progressive ILD compared with those without ILD and healthy controls (Figure 7C). We then confirmed that BAFF directly promotes Bcl-2 expression by naive B cells from CVID patients, doing so at a significantly higher level than the Toll-like receptor 9 (TLR9) agonist unmethylated CpG oligodeoxynucleotides (ODNs) (Figure 7D). These results identify heightened Bcl-2 expression by naive B cells in the lungs and peripheral blood of CVID ILD patients in association with BAFF stimulation via BAFF-R.

Consistent with the role of Bcl-2 in apoptosis inhibition, we found that apoptosis of naive B cells from CVID patients was reduced by addition of BAFF to cultures (Figure 7E). Additionally, we found apoptosis to be largely excluded from the ectopic B cell follicles in progressive CVID ILD lungs, as indicated by the absence of cleaved caspase-3 (Figure 7F). In contrast, apoptosis was diffusely present within B cell follicles in stable ILD patients. These results indicate that BAFF contributes to progression of ILD by impairing apoptosis of naive B cells via BAFF-R.

Lastly, we aimed to confirm BAFF-R as the primary receptor by which BAFF mediates its effects in CVID. One patient in our cohort had biallelic TACI mutations, one allele disrupted by the C104R mutation that alters the extracellular domain and blocks TACI oligomerization and a second allele having the S194X mutation that leads to truncation of TACI that lacks the cytoplasmic signaling domain (39). Despite this biallelic disruption of TACI function, ILD still occurred and the classic features of ectopic B cell follicles found in other CVID ILD patients were seen, including expression of Bcl-2 (Figure 7G). Notably, all 3 TACI-deficient patients in this study had progressive ILD, serum IgM elevations of 10 mg/dl or greater, and elevated serum BAFF levels (Figure 4A). Adding the 3 CVID patients with TACI deficiency in our study cohort to 12 patients with either heterozygous or homozygous TACI mutations (C104R, S194X, or A181E, which also impairs TACI oligomerization) included within the entire medical record at Mount Sinai, we found that the incidence of progressive ILD was markedly greater in those with defects in TACI than in those without (8 of 15 TACI-deficient patients vs. 13 of 71 genetically undefined CVID patients in our cohort, Figure 7H). We also found that CVID patients with pathogenic TACI mutations and ILD had significantly lower levels of isotype-switched memory B cells compared with CVID patients with TACI mutations but without ILD, providing further association of profound B cell maturation arrest with the development of ILD. Together, these results indicate that Bcl-2–mediated apoptosis resistance of naive B cells is driven by BAFF-R and promotes the pulmonary B cell hyperplasia that underlies CVID ILD.

Discussion

Our understanding of CVID pathogenesis has been complicated by the heterogeneous clinical manifestations and lack of genetic etiology in most cases. Even when pathogenic mutations are found, incomplete penetrance and marked variations in phenotype are common in CVID. In contrast to monogenic pediatric immunodeficiencies, adult-onset CVID may have multifactorial etiologies shaped by a merger of genetics with host-microbial influences and sequelae of chronic inflammation. To make sense of this complexity some have attempted to find fundamental pathological features shared among CVID patients with inflammatory complications, such as increased IFN-γ–producing cells or $CD21^{lo}$ B cells (34, 35, 40). In this study, we aimed to identify a shared pathogenic pathway of ILD that transcends the heterogeneity of CVID.

Our work indicates that serum IgM may serve as a biomarker of B cell hyperplasia in CVID, as its level was highest in subjects with more ectopic B cell follicles in the lungs, diminishes with B cell–depletive treatment, and elevates with ILD progression and recurrence after rituximab. We also found serum IgM increase to be associated with ILD in an independent CVID cohort from the USIDNET registry. Higher IgM levels have been associated with lymphoproliferative complications and ILD in CVID as well as decreased survival (6, 7, 11, 28). Moreover, elevated levels of IgM are seen in patients with PI3Kδ gain-of-function mutations leading to a CVID-like disorder with lymphoproliferative lung disease (41). It is important to note that while the IgM levels increased, they remained largely within the

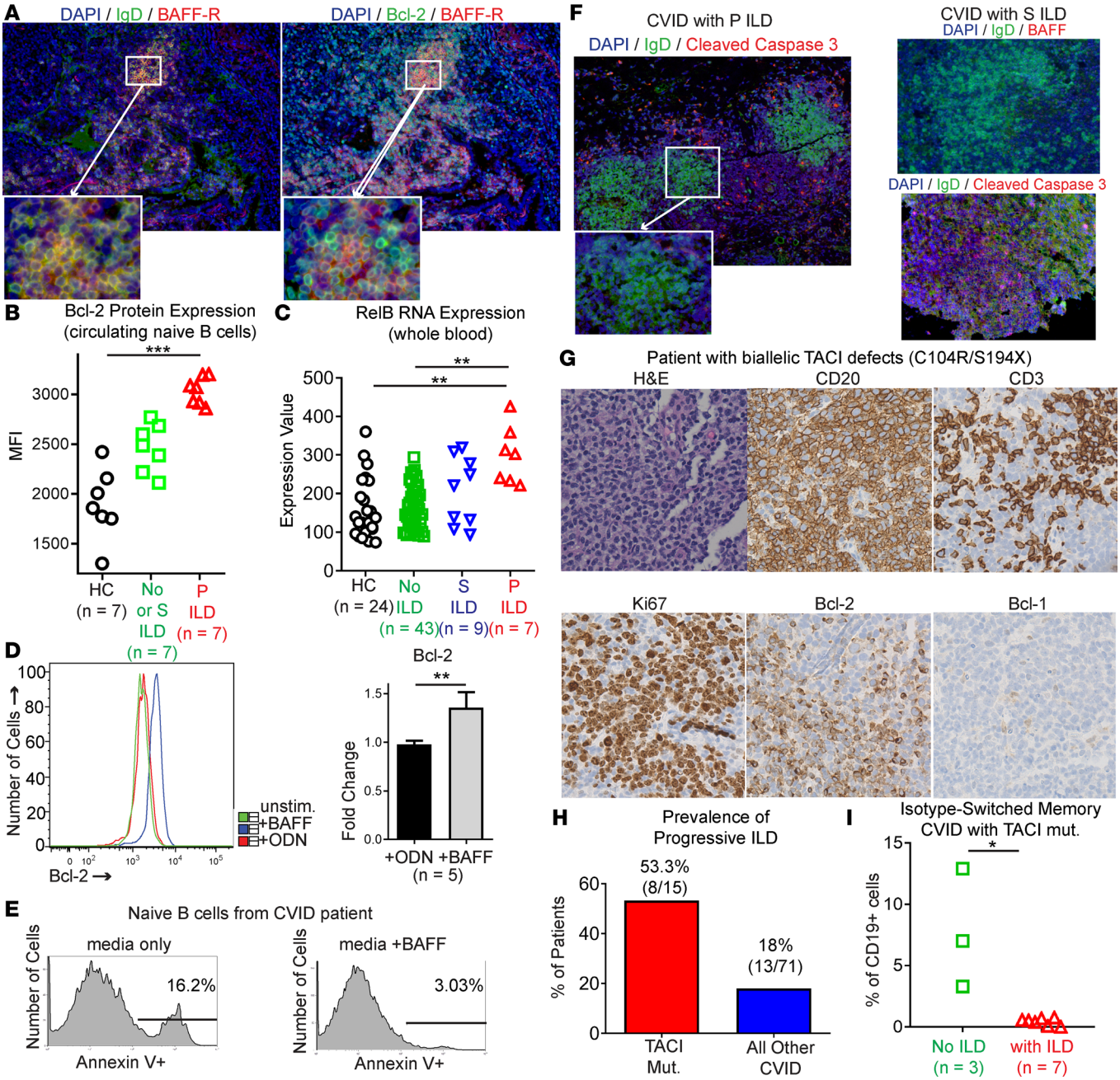

Figure 7. Naive B cells express Bcl-2 in response to BAFF-R signaling to resist apoptosis and promote progression of CVID ILD. (**A**) Serial sections demonstrate that Bcl-2 colocalizes with BAFF-R within ectopic IgD$^+$ B cell follicles in CVID ILD. Original magnification, ×200 and ×400 (insets). (**B**) Bcl-2 expression on circulating naive B cells is elevated in CVID with progressive (P) ILD compared with CVID with stable (S) ILD, no ILD, and healthy controls (HCs). (**C**) RNA expression of the noncanonical NF-κB pathway mediator RelB is elevated in whole blood of CVID patients with P ILD. (**D**) BAFF induces Bcl-2 expression in naive B cells from CVID patients at levels significantly greater than those induced by the TLR9 agonist ODN. (**E**) Addition of BAFF reduces apoptosis in culture of naive B cells from CVID patients. Data representative of 4 similar experiments. (**F**) The pattern of cleaved caspase-3 expression indicates that apoptosis is largely excluded from ectopic B cell follicles in CVID patients with P ILD. In contrast, lung biopsies from CVID patients with S ILD showed extensive apoptosis within ectopic B cell follicles. Data are consistent with results from 6 CVID patients. Original magnification, ×100 and ×200 (insets). (**G**) Biallelic defects of TACI did not prevent lymphoid hyperplasia with prominent Bcl-2–expressing B cell follicles. Original magnification, ×200. (**H**) Incidence of P ILD was higher in CVID patients with genetic deficiency of TACI compared with other CVID patients in our study cohort. (**I**) CVID patients with TACI mutations and ILD had significantly lower levels of isotype-switched memory B cells compared with CVID patients with TACI mutations but no ILD. *$P < 0.05$, **$P < 0.01$, ***$P < 0.001$ by Kruskal-Wallis test for 3-group comparison and Mann-Whitney test for 2-group comparison.

normal reference range (≤ 230 mg/dl). Accordingly, monitoring IgM levels may not detect progression of ILD in individuals that do not have baseline IgM deficiency. The source of IgM in CVID is likely to be short-lived plasmablasts because long-lived plasma cells are absent in these patients. In support of this, we identified IgM$^+$CD27$^+$CD38$^+$ extrafollicular plasmablasts in the lungs of CVID ILD patients

that also expressed CD20, Ki67, and TACI. Additionally, these extrafollicular areas expressed cleaved caspase-3, indicative of apoptosis and these cells being short-lived. As further evidence of plasmablasts as the source of IgM, we found IgM levels to be profoundly reduced by rituximab, a therapy that depletes B cells and plasmablasts but not plasma cells (42).

Our report is the first to our knowledge to show efficacy of rituximab monotherapy in treating CVID ILD. B cell–targeted therapy is efficacious for pathologically similar benign lymphoproliferative lung disease in rheumatoid arthritis and Sjogren's syndrome (43, 44). Rituximab was previously reported to be efficacious in combination with azathioprine for 7 CVID ILD patients; however, comparison with those receiving supportive therapy or rituximab monotherapy was not included (45). Broadly immunosuppressive agents, like azathioprine, can be hepatotoxic, lead to significant gastrointestinal symptoms, promote malignancy, and increase risk of infection, particularly in patients already immunocompromised by CVID (46–49). Furthermore, there is no clear therapeutic endpoint or indication when immunosuppression should be stopped or restarted prior to clinical worsening. Detection of serum IgM increases may be a noninvasive way to identify ILD progression prior to overt pulmonary function decline and allow for more precise usage of B cell–targeted therapy.

We found BAFF to be highest in the blood and lungs of CVID patients with progressive ILD. BAFF increase is also associated with lymphoma, multiple sclerosis, rheumatoid arthritis, Sjogren's syndrome, and SLE (38, 50, 51). BAFF antagonism is used for the treatment of SLE and Sjogren's syndrome and is also used following B cell depletion with rituximab to prevent recurrence of SLE (52–54). BAFF antagonism is yet to be explored in CVID but our results suggest that it may be worth considering in the prevention of ILD progression, especially given its preferable safety profile compared with other immunosuppressive agents (55, 56).

We found elevation of IFN-γ in progression of CVID ILD, correlation of STAT1 and BAFF RNA expression levels, and that IFN-γ promotes BAFF production by PBMCs at higher levels in CVID ILD patients. $CD14^+$ monocytes are the major leukocyte responding to IFN-γ in CVID ILD on the basis of p-STAT1 expression, which was significantly elevated in those with progressive ILD. In concordance with their heightened response to IFN-γ, $CD14^+$ monocytes were the most prevalent BAFF-producing cell in CVID ILD and had elevated expression of BAFF in those with progressive ILD. The stimulus for the heightened IFN-γ production in CVID that drives BAFF production remains undefined. Bacterial translocation has been described in CVID and may be a driving force for IFN-γ, but this remains to be further explored (57).

Differences in expression of BAFF-R, TACI, and BCMA during B cell maturation could have implications for disease pathogenesis. We found $BAFF\text{-}R^+$ naive and transitional B cell subsets to predominate in the blood and lungs of CVID ILD patients. This finding is consistent with the B cell maturation defect inherent to CVID as well as findings of previous groups that noted that isotype-switched memory B cells are lowest in CVID patients with lung disease (58, 59). The ectopic B cell follicles we uncovered to be a key part of CVID ILD pathogenesis were made up of $BAFF\text{-}R^+IgD^+CD27^-$ naive B cells. Naive B cells can contribute to disease in significant ways, particularly in conditions in which BAFF is elevated. For example, naive B cells are an important source of pathogenic antibodies in SLE (60).

The unique role of BAFF-R among the 3 BAFF receptors in signaling via the noncanonical NF-κB pathway may allow this receptor to have a prominent role in promoting autoreactivity and lymphoproliferation of naive B cells through expression of Bcl-2 family prosurvival factors (61). Indeed, we found expression of Bcl-2 in pulmonary B cell follicles and increased Bcl-2 in circulating naive B cells from progressive CVID ILD patients. Induction by BAFF in naive CVID B cells occurred in conjunction with apoptosis inhibition, providing evidence for BAFF-R and its noncanonical NF-κB signaling in pathogenesis of CVID ILD. The fact that TACI deficiency increased incidence of progressive ILD in CVID patients is even further suggestive that BAFF and BAFF-R are contributing to disease. TACI-deficient patients are known to have an increased rate of autoimmunity and lymphoproliferative disease in CVID (62, 63), in association with increased autoreactive B cell selection and survival (64). BCMA and TACI may compete for ligand and/or provide signals that regulate the effects of BAFF-R. Thus, deficiency of these 2 receptors may exacerbate BAFF-R–driven survival mechanisms that lead to the B cell hyperplasia underlying CVID ILD (65, 66).

CVID is a heterogeneous disorder with diverse clinical manifestations that include ILD that undergoes acute periods of progression for reasons not understood. Our study identified BAFF-driven B cell hyperplasia as underlying CVID ILD progression in association with serum IgM elevation reflecting the extent of ILD progression. Harnessing the B cell maturation and TACI defects in CVID, we also demonstrated that BAFF-R functions distinctly from TACI and BCMA to mediate B cell hyperplasia via Bcl-2 induction and resultant apoptosis inhibition. Building upon these results, subsequent studies should explore the clinical

utility of serum IgM measurement as a noninvasive biomarker to guide the usage of B cell–depletive therapy as well as BAFF and other B cell survival pathways as targets to prevent disease recurrence without the adverse effects of broader immunosuppressive therapies.

Methods

Subjects and retrospective review of electronic medical records. All subjects recruited for this study were patients at the Mount Sinai Clinical Immunology Faculty Practice. Electronic medical records were reviewed retrospectively for patient encounters from January 1, 2003 until July 1, 2018. Patients with the International Classification of Diseases Ninth or Tenth Revision Code for CVID (279.06 or D83.9) and CT scan of the chest or documentation in the medical record of absence of lung disease was included. CVID patients were determined to have ILD if the chest CT showed ground-glass opacity and/or more than 4 nodules of at least 1 mm in diameter as well as pathological diagnosis of ILD, if available (11). To be included in this study, CVID ILD patients had to have FVC and/or DLCO measurements conducted 24 months apart. The diagnosis of CVID was confirmed in all subjects based on markedly low serum IgG and IgA and/or IgM levels (IgG < 400 mg/dl, IgA < 45 mg/dl, IgM < 35 mg/dl), poor response to at least one vaccine, and exclusion of other causes of hypogammaglobulinemia (1). Patient age, sex, FVC, DLCO, laboratory values (IgG, IgA, IgM, complete blood count with differential, lymphocyte subsets), chest CT radiologist report, and pathologist report of lung biopsy were derived from the medical record. History of bronchiectasis was confirmed by CT scan review or radiology report. History of ITP or other autoimmunity was determined from coding or notation in the medical record. Rituximab was administered at 375 mg/m^2 for 4 weekly doses. A query was submitted to the USIDNET registry, a program of the Immune Deficiency Foundation (IDF), supported by a cooperative agreement, U24AI86837, from the National Institute of Allergy and Infectious Diseases (NIAID) requesting the following data from CVID patients: demographics (excluding Mount Sinai patients), respiratory conditions, and Ig levels measured at least 6 or more months apart. Patients with a diagnosis of CVID were included in the analysis if they had an IgA and/or IgM value that was less than 2 standard deviations below the standard mean for age; for adults we used an IgA less than 70 mg/dl and IgM less than 40 mg/dl. If the subject from the USIDNET registry had one of the following diagnoses they were listed as having ILD in our analysis: diffuse infiltrative lung disease, follicular bronchiolitis, interstitial lung disease, interstitial pneumonia, lymphoid interstitial pneumonia, multiple nodules of lung, pulmonary granuloma, pulmonary nodular lymphoid hyperplasia, respiratory bronchiolitis–associated interstitial lung disease, and restrictive lung disease.

Lung biopsies and immunofluorescence. All biopsies were conducted as part of routine clinical care of CVID patients with symptoms and CT findings suggestive of lung disease. All CVID ILD patients included in the study had ILD diagnoses from board-certified pathologists consistent with forms of pulmonary lymphoid hyperplasia: follicular bronchiolitis, lymphocytic interstitial pneumonia, or nodular lymphoid hyperplasia. Formalin-fixed, paraffin-embedded tissue sections from lung biopsies were utilized for all immunohistochemical or immunofluorescence studies. Hematoxylin and eosin staining as well as immunohistochemical identification of CD3, CD20, CD23, Bcl6, and Ki67 were done as part of standard patient care. Appropriate positive and negative controls were reviewed. The number of ectopic B cell follicles in 6,000-μm by 3,000-μm lung sections was quantified by a board-certified pathologist who was blinded to the subject's identity and serum IgM level. For immunofluorescence staining, tissue sections of 5-μm thickness were stained with primary antibodies (Supplemental Table 1) and appropriate secondary reagents conjugated with Alex Fluor 488, 546, 647, or cyanine 5–conjugated streptavidin (Jackson ImmunoResearch Laboratories). Nuclei were visualized with 4,6-diamidino-2-phenylindole (DAPI). Primary antibodies with irrelevant binding activity and appropriate secondary reagents were used to validate the specificity of tissue staining. Images were acquired with a Zeiss Axioplan 2 microscope (Atto Instruments). IgM$^+$ cells and DAPI nuclei were quantified using CellProfiler software in 440-μm by 330-μm lung sections (2,000 by 1,500 pixels) imaged by ×20 objective lens.

APRIL, BAFF, and IFN-γ measurement. Nunc MaxiSorp 96-well plates were coated with APRIL or BAFF capture antibodies (R&D Systems) overnight at 4°C. Plates were then washed with PBS/0.05% Tween 20, blocked for at least 30 minutes at room temperature with PBS/0.5% BSA, washed again, and then incubated with serum for 90 minutes at room temperature. Plates were then washed and incubated with HRP-conjugated APRIL or BAFF detection antibodies for 90 minutes. After final washes, plates were developed with TMB substrate (BD Biosciences), with 2N H_2SO_4 (Sigma-Aldrich) added once fully developed. Absorbance of wells was measured at an optical density (OD) of 450 nm by a POLARstar Omega plate reader (BMG Labtech). Plasma

IFN-γ was measured using a Luminex multiplex assay that uses micron-sized color-coded magnetic bead sets coated with a special mixture of dyes to quantify samples. This assay was done at the Human Immune Monitoring Center at Mount Sinai, which houses and runs the assay on the Luminex 200 system.

Cell culture. PBMCs were purified from fresh venous blood using Ficoll density gradient centrifugation. To stimulate BAFF production, PBMCs were incubated in 96-well plates at a concentration of 5×10^5 cells/200 μl in RPMI 1640/antibiotic-antimycotic (Gibco) and 10% FBS (Atlanta Biologicals) and stimulated with or without 10 ng/ml IFN-γ (R&D Systems) for 18 hours. For Bcl-2 and annexin V measurement by flow cytometry, B cells were isolated from PBMCs using negative selection magnetic beads (Miltenyi Biotec) and cultured in 96-well plates at a concentration of 5×10^5 cells/200 μl in RPMI 1640/antibiotic-antimycotic and 10% FBS and stimulated with or without 100 ng/ml BAFF (R&D Systems) or 1 μg/ml CPG ODN (InvivoGen) for 18 hours.

Flow cytometry. Flow cytometry analysis of PBMCs was conducted using the multicolor flow cytometer LSR II (BD Biosciences) and FloJo analysis software (Tree Star). The fluorescein-conjugated antibodies used to detect CD3 (clone APA1/1), CD14 (M5E2), CD11c (B-ly6), CD16 (3G8), CD19 (SJ25C1), CD27 (M-T271), IgM (G201-127), IgD (IA6-2), CD21 (B-ly4), BAFF-R (11C1), and TACI (1A1) were all from BD Biosciences and CD38 (HB-7) was from Biolegend. Measurement of intracellular Bcl-2 (Bcl-2/100, BD Biosciences) or BAFF (7H22-E16, BD Biosciences) was done after fixation and permeabilization of cells. Annexin V staining was conducted as per the manufacturer's protocol (BD Biosciences). $CD14^+$ monocytes in peripheral blood were defined as $CD3^-CD19^-$, and $CD11c^+$ dendritic cells in peripheral blood were defined as $lineage^-$ ($CD3^-CD14^-CD16^-CD19^-$).

Mass cytometry. Whole blood from 10 CVID patients with progressive ILD, 10 CVID patients with stable or no ILD, and 10 healthy controls was stimulated for 20 minutes with 10 μg/ml IFN-γ and then fixed with Smart Tube buffer (Smart Tube, Inc.) for batched mass cytometry analysis. Samples were thawed and barcoded in batches of 10 samples using palladium barcoding reagents, and then incubated in a cocktail of surface-binding antibodies to identify major immune cell subsets. The marker expression assigned to each leukocyte subset is summarized in Supplemental Figure 4. The cells were then fixed, permeabilized, and stained with antibodies against intracellular cytokines and transcription factors (Supplemental Table 2). All antibodies were purchased preconjugated to metal tags or conjugated in house by using MaxPar X8 conjugation kits (Fluidigm). Samples were then postfixed and stained with iridium nucleic acid intercalator (Fluidigm), and then washed and data acquired on a Helios mass cytometer (Fluidigm). Following acquisition, the barcoded samples were normalized, demultiplexed, and debris and normalization beads were manually excluded. $Ir191/193^+$ cell events were analyzed using both Cytobank and the Astrolabe Cytometry Platform (Astrolabe Diagnostics, Inc.). Cells were clustered using SPADE and FlowSOM clustering (67). Differential abundance analysis was done using the edgeR R package (68, 69) following a previously outlined method (70). Cell subset definitions follow that done previously (71, 72). Cluster labeling, method implementation, and visualization were done through the Astrolabe Platform.

Statistics. For clinical and laboratory data derived from the electronic medical record, categorical values were compared using the χ^2 test and continuous values were compared using the Kruskal-Wallis test. Mann-Whitney testing was utilized to assess statistical significance for 2-group comparisons, Kruskal-Wallis test was used for multiple group comparisons except for p-STAT1 and leukocyte subsets by mass cytometry, for which 2-way ANOVA with Tukey's multiple comparisons test was used. If the Kruskal-Wallis test yielded a P value of less than 0.05, differences between subject groups were assessed using Dunn's multiple comparisons test. Calculations were made using Prism software (GraphPad). A P value less than 0.05 was considered significant.

Study approval. This study was approved by the institutional review board of the Icahn School of Medicine at Mount Sinai and was carried out in accordance with the Code of Ethics of the World Medical Association (Declaration of Helsinki). Written informed consent was received from participants prior to inclusion in the study.

Author contributions

PJM conceived the project, designed and performed research, analyzed and discussed data, prepared the figures, and wrote the manuscript. GG, MC, HMK, TW, LR, BHL, and AHR performed experiments and analyzed and discussed data. EKG, AC, and CCR analyzed and discussed data and the research plan. All authors contributed towards critical revision of the manuscript and approved the final draft.

Acknowledgments

We thank the patients and their families for their participation in this research as well as the nursing staff for sharing in the care of these patients. This work was supported by grants from the Primary Immune Deficiency Treatment Consortium, Rare Disease Foundation, NIH grants AI137183 (to PJM) and AI061093 (to CCR), and the Swedish Research Council and Swedish Society of Medicine grant 2015-06486 (to EKG). Flow cytometry was performed at the Flow Cytometry CoRE, microscopy and image analysis was performed at the Microscopy CoRE, and mass cytometry was done at the Human Immune Monitoring Center of the Icahn School of Medicine at Mount Sinai using mass cytometry instrumentation supported by instrumentation grant S10OD023547.

Address correspondence to: Paul J. Maglione, Boston University School of Medicine, Pulmonary Center, 72 East Concord Street, R304, Boston, Massachusetts 02118, USA. Phone: 617.358.0913; Email: pmaglion@bu.edu.

MC's present address is: Immunology Program, Memorial Sloan Kettering Cancer Center, New York, New York, USA.

1. Cunningham-Rundles C, Maglione PJ. Common variable immunodeficiency. *J Allergy Clin Immunol*. 2012;129(5):1425–1426.e3.
2. Warnatz K, et al. Severe deficiency of switched memory B cells (CD27(+)IgM(-)IgD(-)) in subgroups of patients with common variable immunodeficiency: a new approach to classify a heterogeneous disease. *Blood*. 2002;99(5):1544–1551.
3. Taubenheim N, et al. Defined blocks in terminal plasma cell differentiation of common variable immunodeficiency patients. *J Immunol*. 2005;175(8):5498–5503.
4. Kienzler AK, Hargreaves CE, Patel SY. The role of genomics in common variable immunodeficiency disorders. *Clin Exp Immunol*. 2017;188(3):326–332.
5. Cunningham-Rundles C. The many faces of common variable immunodeficiency. *Hematology Am Soc Hematol Educ Program*. 2012;2012:301–305.
6. Chapel H, et al. Common variable immunodeficiency disorders: division into distinct clinical phenotypes. *Blood*. 2008;112(2):277–286.
7. Resnick ES, Moshier EL, Godbold JH, Cunningham-Rundles C. Morbidity and mortality in common variable immune deficiency over 4 decades. *Blood*. 2012;119(7):1650–1657.
8. Rider NL, et al. Health-related quality of life in adult patients with common variable immunodeficiency disorders and impact of treatment. *J Clin Immunol*. 2017;37(5):461–475.
9. Carrillo J, Restrepo CS, Rosado de Christenson M, Ojeda Leon P, Lucia Rivera A, Koss MN. Lymphoproliferative lung disorders: a radiologic-pathologic overview. Part I: Reactive disorders. *Semin Ultrasound CT MR*. 2013;34(6):525–534.
10. Bates CA, Ellison MC, Lynch DA, Cool CD, Brown KK, Routes JM. Granulomatous-lymphocytic lung disease shortens survival in common variable immunodeficiency. *J Allergy Clin Immunol*. 2004;114(2):415–421.
11. Maglione PJ, Overbey JR, Radigan L, Bagiella E, Cunningham-Rundles C. Pulmonary radiologic findings in common variable immunodeficiency: clinical and immunological correlations. *Ann Allergy Asthma Immunol*. 2014;113(4):452–459.
12. Tian X, Yi ES, Ryu JH. Lymphocytic interstitial pneumonia and other benign lymphoid disorders. *Semin Respir Crit Care Med*. 2012;33(5):450–461.
13. Guinee DG. Update on nonneoplastic pulmonary lymphoproliferative disorders and related entities. *Arch Pathol Lab Med*. 2010;134(5):691–701.
14. Schussler E, Beasley MB, Maglione PJ. Lung disease in primary antibody deficiencies. *J Allergy Clin Immunol Pract*. 2016;4(6):1039–1052.
15. Verma N, Grimbacher B, Hurst JR. Lung disease in primary antibody deficiency. *Lancet Respir Med*. 2015;3(8):651–660.
16. Schubert D, et al. Autosomal dominant immune dysregulation syndrome in humans with CTLA4 mutations. *Nat Med*. 2014;20(12):1410–1416.
17. Gámez-Díaz L, et al. The extended phenotype of LPS-responsive beige-like anchor protein (LRBA) deficiency. *J Allergy Clin Immunol*. 2016;137(1):223–230.
18. Milner JD, et al. Early-onset lymphoproliferation and autoimmunity caused by germline STAT3 gain-of-function mutations. *Blood*. 2015;125(4):591–599.
19. Maglione PJ. Autoimmune and lymphoproliferative complications of common variable immunodeficiency. *Curr Allergy Asthma Rep*. 2016;16(3):19.
20. Maglione PJ, Ko HM, Beasley MB, Strauchen JA, Cunningham-Rundles C. Tertiary lymphoid neogenesis is a component of pulmonary lymphoid hyperplasia in patients with common variable immunodeficiency. *J Allergy Clin Immunol*. 2014;133(2):535–542.
21. Aghamohammadi A, et al. Comparison of pulmonary diseases in common variable immunodeficiency and X-linked agammaglobulinaemia. *Respirology*. 2010;15(2):289–295.
22. Mackay F, Schneider P. Cracking the BAFF code. *Nat Rev Immunol*. 2009;9(7):491–502.
23. Knight AK, Radigan L, Marron T, Langs A, Zhang L, Cunningham-Rundles C. High serum levels of BAFF, APRIL, and TACI in common variable immunodeficiency. *Clin Immunol*. 2007;124(2):182–189.
24. Barbosa RR, et al. Reduced BAFF-R and increased TACI expression in common variable immunodeficiency. *J Clin Immunol*. 2014;34(5):573–583.

25. Polverino F, et al. B cell-activating factor. An orchestrator of lymphoid follicles in severe chronic obstructive pulmonary disease. *Am J Respir Crit Care Med*. 2015;192(6):695–705.
26. Seys LJ, et al. Role of B cell-activating factor in chronic obstructive pulmonary disease. *Am J Respir Crit Care Med*. 2015;192(6):706–718.
27. Raghu G, et al. An official ATS/ERS/JRS/ALAT statement: idiopathic pulmonary fibrosis: evidence-based guidelines for diagnosis and management. *Am J Respir Crit Care Med*. 2011;183(6):788–824.
28. Maglione PJ, Overbey JR, Cunningham-Rundles C. Progression of common variable immunodeficiency interstitial lung disease accompanies distinct pulmonary and laboratory findings. *J Allergy Clin Immunol Pract*. 2015;3(6):941–950.
29. Maffucci P, et al. Genetic diagnosis using whole exome sequencing in common variable immunodeficiency. *Front Immunol*. 2016;7:220.
30. Carter LM, Isenberg DA, Ehrenstein MR. Elevated serum BAFF levels are associated with rising anti-double-stranded DNA antibody levels and disease flare following B cell depletion therapy in systemic lupus erythematosus. *Arthritis Rheum*. 2013;65(10):2672–2679.
31. Cornec D, et al. Blood and salivary-gland BAFF-driven B-cell hyperactivity is associated to rituximab inefficacy in primary Sjögren's syndrome. *J Autoimmun*. 2016;67:102–110.
32. Naradikian MS, Perate AR, Cancro MP. BAFF receptors and ligands create independent homeostatic niches for B cell subsets. *Curr Opin Immunol*. 2015;34:126–129.
33. Park J, et al. Interferon signature in the blood in inflammatory common variable immune deficiency. *PLoS ONE*. 2013;8(9):e74893.
34. Cols M, et al. Expansion of inflammatory innate lymphoid cells in patients with common variable immune deficiency. *J Allergy Clin Immunol*. 2016;137(4):1206–1215.e6.
35. Unger S, et al. The TH1 phenotype of follicular helper T cells indicates an IFN-γ-associated immune dysregulation in patients with CD21low common variable immunodeficiency. *J Allergy Clin Immunol*. 2018;141(2):730–740.
36. Litinskiy MB, et al. DCs induce CD40-independent immunoglobulin class switching through BLyS and APRIL. *Nat Immunol*. 2002;3(9):822–829.
37. Lehtonen A, Matikainen S, Julkunen I. Interferons up-regulate STAT1, STAT2, and IRF family transcription factor gene expression in human peripheral blood mononuclear cells and macrophages. *J Immunol*. 1997;159(2):794–803.
38. Yang S, Li JY, Xu W. Role of BAFF/BAFF-R axis in B-cell non-Hodgkin lymphoma. *Crit Rev Oncol Hematol*. 2014;91(2):113–122.
39. He B, et al. The transmembrane activator TACI triggers immunoglobulin class switching by activating B cells through the adaptor MyD88. *Nat Immunol*. 2010;11(9):836–845.
40. Rakhmanov M, et al. Circulating CD21low B cells in common variable immunodeficiency resemble tissue homing, innate-like B cells. *Proc Natl Acad Sci USA*. 2009;106(32):13451–13456.
41. Lucas CL, et al. Dominant-activating germline mutations in the gene encoding the PI(3)K catalytic subunit p110δ result in T cell senescence and human immunodeficiency. *Nat Immunol*. 2014;15(1):88–97.
42. Hofmann K, Clauder AK, Manz RA. Targeting B cells and plasma cells in autoimmune diseases. *Front Immunol*. 2018;9:835.
43. Chen MH, Chen CK, Chou HP, Chen MH, Tsai CY, Chang DM. Rituximab therapy in primary Sjögren's syndrome with interstitial lung disease: a retrospective cohort study. *Clin Exp Rheumatol*. 2016;34(6):1077–1084.
44. Md Yusof MY, et al. Effect of rituximab on the progression of rheumatoid arthritis-related interstitial lung disease: 10 years' experience at a single centre. *Rheumatology (Oxford)*. 2017;56(8):1348–1357.
45. Chase NM, et al. Use of combination chemotherapy for treatment of granulomatous and lymphocytic interstitial lung disease (GLILD) in patients with common variable immunodeficiency (CVID). *J Clin Immunol*. 2013;33(1):30–39.
46. de Jong DJ, Goullet M, Naber TH. Side effects of azathioprine in patients with Crohn's disease. *Eur J Gastroenterol Hepatol*. 2004;16(2):207–212.
47. Vögelin M, et al. The impact of azathioprine-associated lymphopenia on the onset of opportunistic infections in patients with inflammatory bowel disease. *PLoS ONE*. 2016;11(5):e0155218.
48. Chien SH, et al. Use of azathioprine for graft-vs-host disease is the major risk for development of secondary malignancies after haematopoietic stem cell transplantation: a nationwide population-based study. *Br J Cancer*. 2015;112(1):177–184.
49. Chertoff J, Alam S, Black M, Elgendy IY. Azathioprine-induced hepatitis and cholestasis occurring 1 year after treatment. *BMJ Case Rep*. 2014.
50. Moura RA, et al. BAFF and TACI gene expression are increased in patients with untreated very early rheumatoid arthritis. *J Rheumatol*. 2013;40(8):1293–1302.
51. Steri M, et al. Overexpression of the cytokine BAFF and autoimmunity risk. *N Engl J Med*. 2017;376(17):1615–1626.
52. Kraaij T, Huizinga TW, Rabelink TJ, Teng YK. Belimumab after rituximab as maintenance therapy in lupus nephritis. *Rheumatology (Oxford)*. 2014;53(11):2122–2124.
53. Marcondes F, Scheinberg M. Belimumab in the treatment of systemic lupus erythematous: An evidence based review of its place in therapy. *Autoimmun Rev*. 2018;17(2):103–107.
54. Nocturne G, Cornec D, Seror R, Mariette X. Use of biologics in Sjögren's syndrome. *Rheum Dis Clin North Am*. 2016;42(3):407–417.
55. Bruce IN, et al. Long-term organ damage accrual and safety in patients with SLE treated with belimumab plus standard of care. *Lupus*. 2016;25(7):699–709.
56. De Vita S, et al. Efficacy and safety of belimumab given for 12 months in primary Sjögren's syndrome: the BELISS open-label phase II study. *Rheumatology (Oxford)*. 2015;54(12):2249–2256.
57. Perreau M, et al. Exhaustion of bacteria-specific CD4 T cells and microbial translocation in common variable immunodeficiency disorders. *J Exp Med*. 2014;211(10):2033–2045.
58. Detková D, et al. Common variable immunodeficiency: association between memory B cells and lung diseases. *Chest*. 2007;131(6):1883–1889.
59. Maarschalk-Ellerbroek LJ, et al. CT screening for pulmonary pathology in common variable immunodeficiency disorders and

the correlation with clinical and immunological parameters. *J Clin Immunol*. 2014;34(6):642–654.
60. Tipton CM, et al. Diversity, cellular origin and autoreactivity of antibody-secreting cell population expansions in acute systemic lupus erythematosus. *Nat Immunol*. 2015;16(7):755–765.
61. Carrington EM, Tarlinton DM, Gray DH, Huntington ND, Zhan Y, Lew AM. The life and death of immune cell types: the role of BCL-2 anti-apoptotic molecules. *Immunol Cell Biol*. 2017;95(10):870–877.
62. Salzer U, et al. Mutations in TNFRSF13B encoding TACI are associated with common variable immunodeficiency in humans. *Nat Genet*. 2005;37(8):820–828.
63. Zhang L, et al. Transmembrane activator and calcium-modulating cyclophilin ligand interactor mutations in common variable immunodeficiency: clinical and immunologic outcomes in heterozygotes. *J Allergy Clin Immunol*. 2007;120(5):1178–1185.
64. Romberg N, et al. CVID-associated TACI mutations affect autoreactive B cell selection and activation. *J Clin Invest*. 2013;123(10):4283–4293.
65. Seshasayee D, Valdez P, Yan M, Dixit VM, Tumas D, Grewal IS. Loss of TACI causes fatal lymphoproliferation and autoimmunity, establishing TACI as an inhibitory BLyS receptor. *Immunity*. 2003;18(2):279–288.
66. Sanchez E, et al. The role of B-cell maturation antigen in the biology and management of, and as a potential therapeutic target in, multiple myeloma. *Target Oncol*. 2018;13(1):39–47.
67. Van Gassen S, et al. FlowSOM: Using self-organizing maps for visualization and interpretation of cytometry data. *Cytometry A*. 2015;87(7):636–645.
68. Robinson MD, McCarthy DJ, Smyth GK. edgeR: a Bioconductor package for differential expression analysis of digital gene expression data. *Bioinformatics*. 2010;26(1):139–140.
69. McCarthy DJ, Chen Y, Smyth GK. Differential expression analysis of multifactor RNA-Seq experiments with respect to biological variation. *Nucleic Acids Res*. 2012;40(10):4288–4297.
70. Lun ATL, Richard AC, Marioni JC. Testing for differential abundance in mass cytometry data. *Nat Methods*. 2017;14(7):707–709.
71. Maecker HT, McCoy JP, Nussenblatt R. Standardizing immunophenotyping for the Human Immunology Project. *Nat Rev Immunol*. 2012;12(3):191–200.
72. Finak G, et al. Standardizing flow cytometry immunophenotyping analysis from the Human ImmunoPhenotyping Consortium. *Sci Rep*. 2016;6:20686.